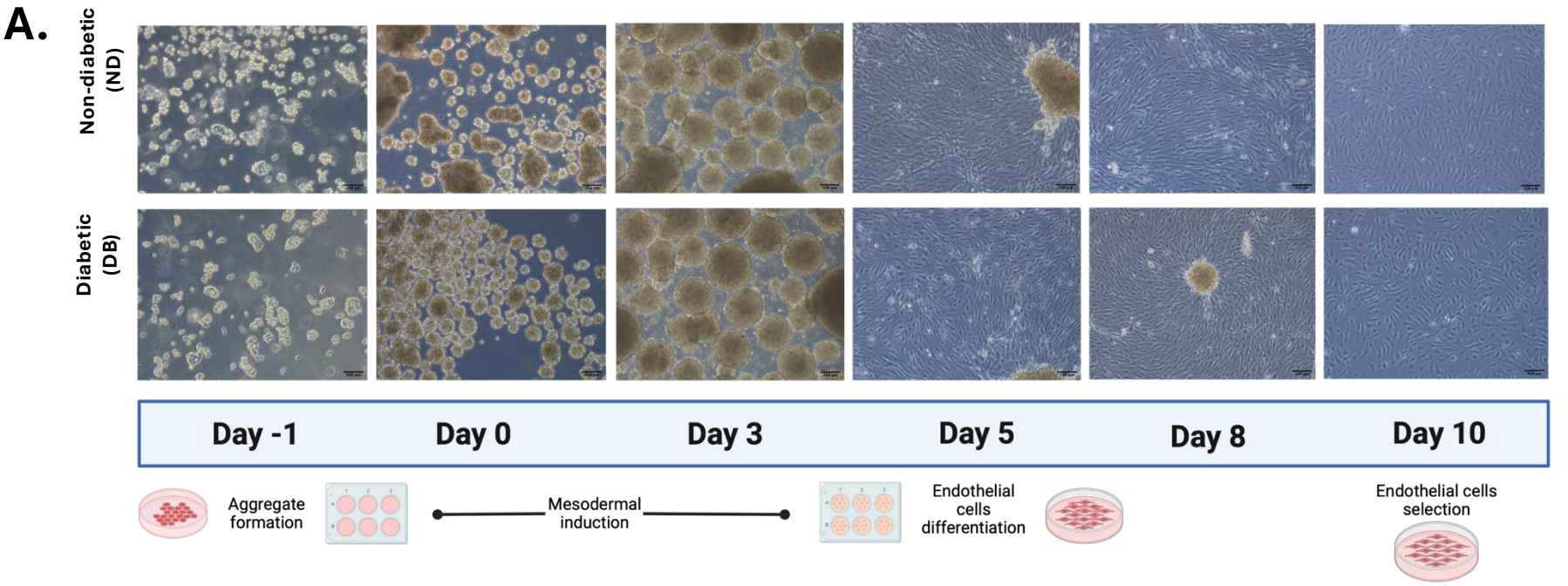

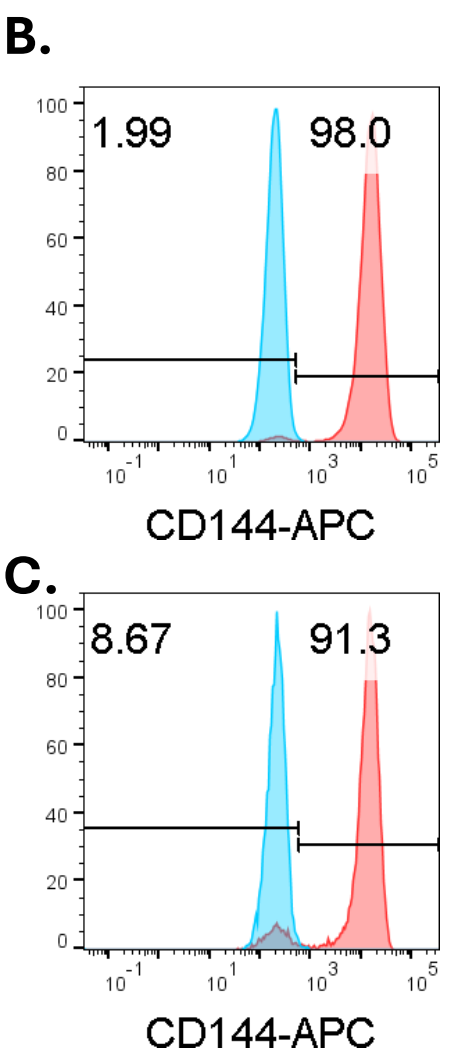

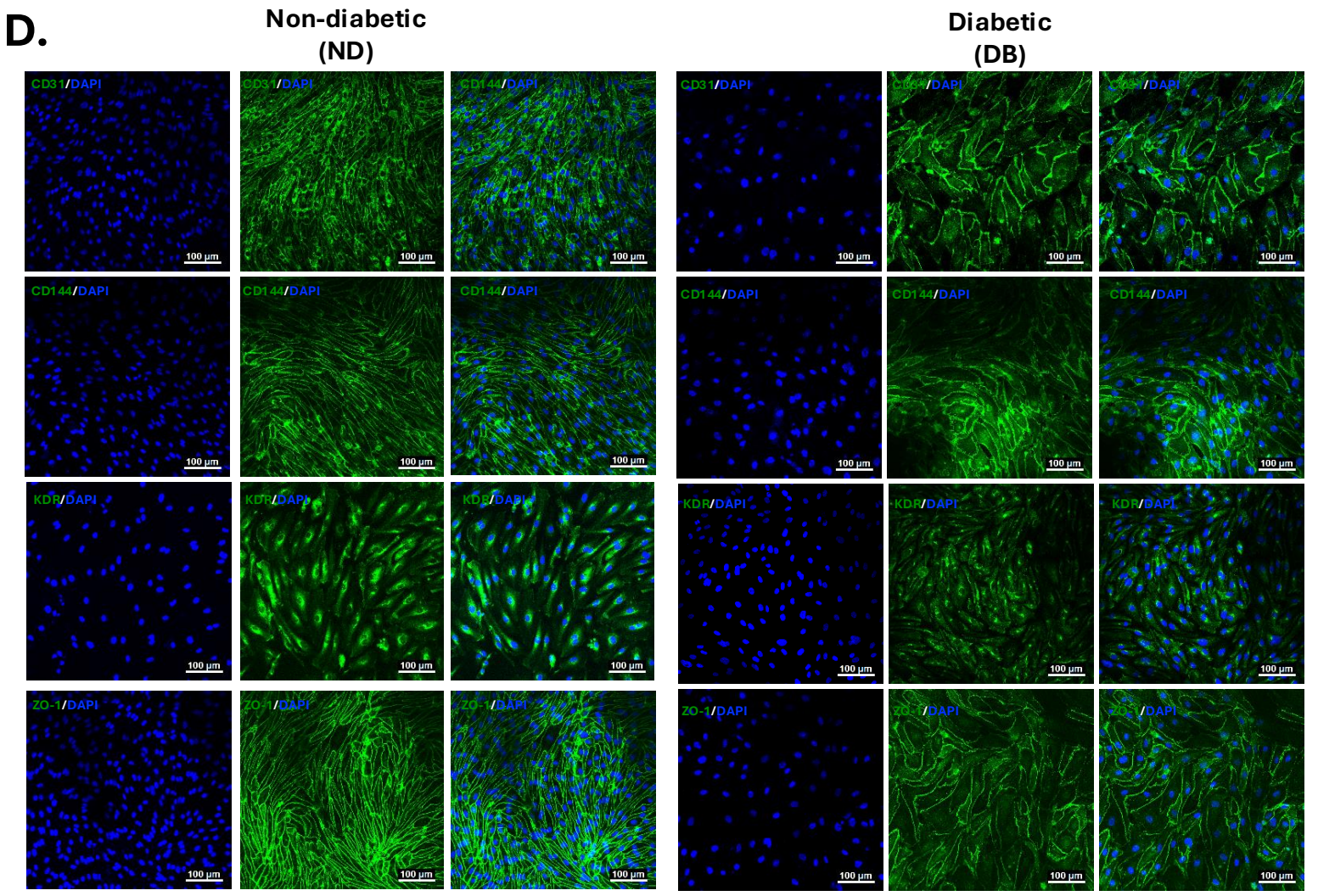

Supplementary figure 1. Differentiation and Characterization of Endothelial Cells Derived from Human iPSCs (hiPSCs).
(A) Schematic representation of the endothelial cell differentiation process from hiPSCs, completed within 10 days.
(B, C) Quantification of differentiation efficiency in endothelial cells derived from non-diabetic **(B)** and diabetic **(C)** donors before magnetic-activated cell sorting (autoMACS) selection, showing a high efficiency of 90–98%.
(D) Immunofluorescence staining of endothelial markers (CD31, CD144, KDR, and ZO-1) in iPSC-derived endothelial cells (iPS-ECs), demonstrating strong expression localized at the cell junctions, confirming endothelial identity.
Imaging Details: Magnification: 20×; Scale bar: 100 µm.

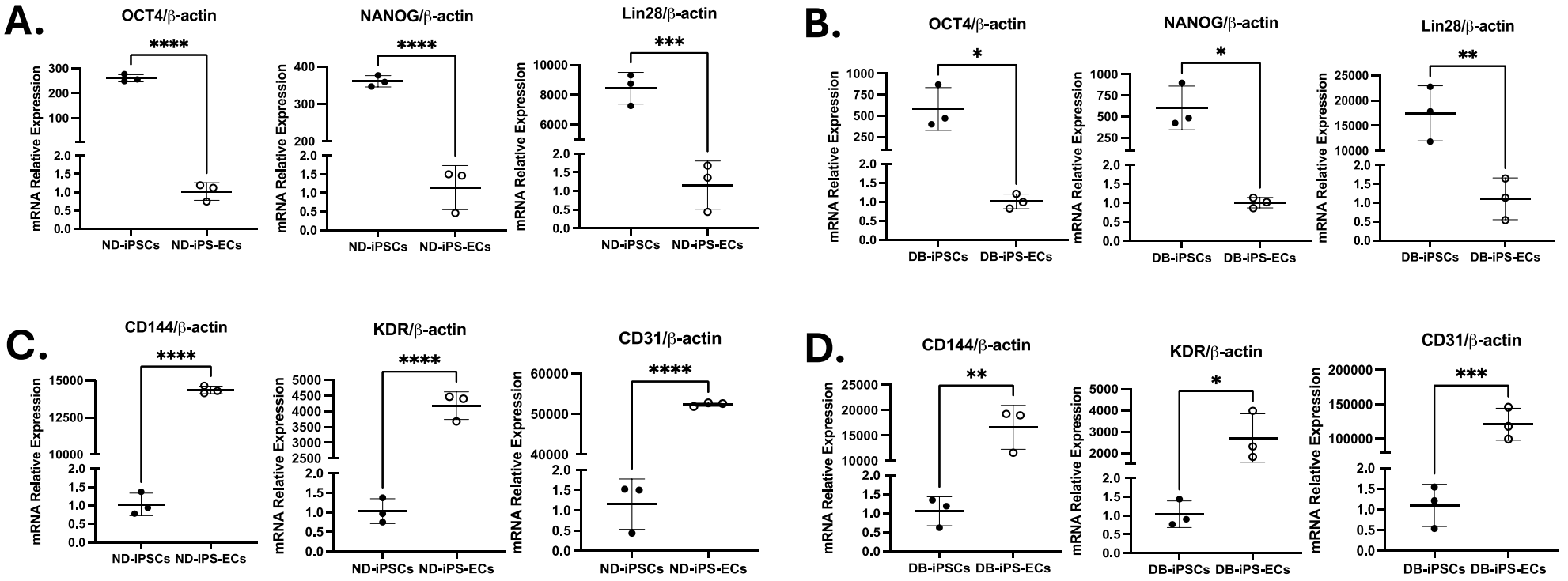

Supplementary figure 2. The iPS-ECs derived from non-diabetic (ND) and diabetic (DB) donors exhibit significant upregulation of endothelial cell markers and are capable of forming tube-like structures. The mRNA levels of pluripotency markers were notably high in the iPSCs from both ND **(A)** and DB **(B)** groups. Upon differentiation into endothelial cells (iPS-ECs), the mRNA expression of pluripotency markers was ablated, while the expression of endothelial cell markers was significantly enhanced **(C and D)**. Western blot analysis showed that pluripotency markers, including OCT4 and NANOG, were strongly expressed in the iPSCs from both ND and DB groups. However, as the iPSCs differentiated into iPS-ECs, the levels of these markers decreased, and the endothelial markers, such as CD31 and CD144, were upregulated. Functional assays (D) demonstrated that iPS-ECs were capable of forming tube-like structures. Statistical analysis was performed using a Student's t-test.

Imaging Details: Magnification: 5X.

Statistical Significance: Statistical analysis was tested by Kruskall-Wallis or One-Way ANOVA, ✻ = p<0.05; ✻✻ = p<0.01; ✻✻✻✻ = p<0.0001.

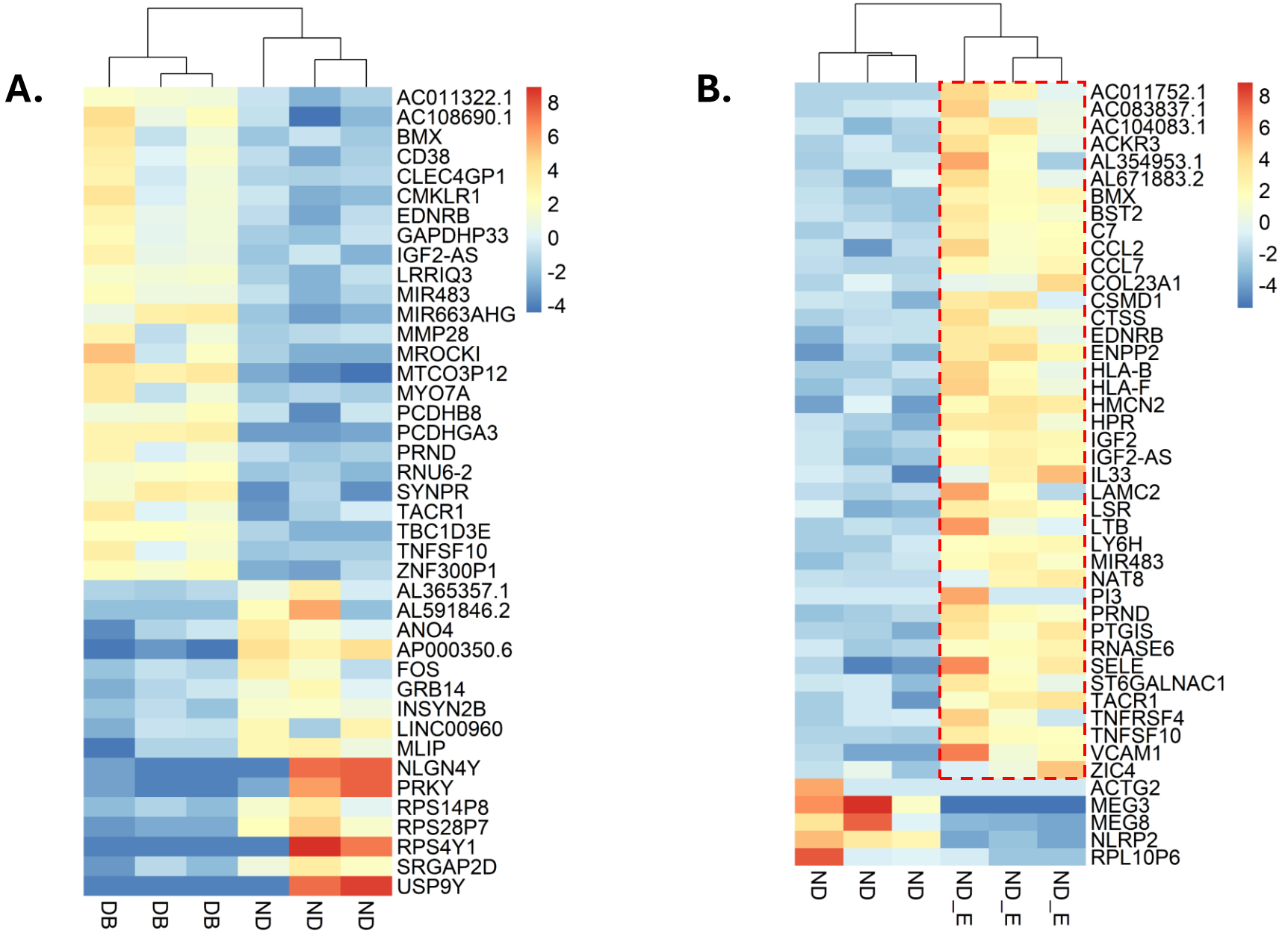

Supplementary Figure 3. As consequence of *E. coli* infection, the endothelial cells derived from donors with non-diabetes (NDE) and with diabetes (DBE) exhibits inflammation. Heatmaps of RNA-seq data showed 40 top differentially expressed genes (DEGs) across four pairwise comparisons **A.** DB vs ND. **B.** NDE vs ND. **C.** DBE vs DB. **D.** DBE vs NDE groups with cut-off log2 FC>5/FC<-5 and FDR <0.01. The red colour indicated the upregulated whilst the blue colour represented the downregulated genes.

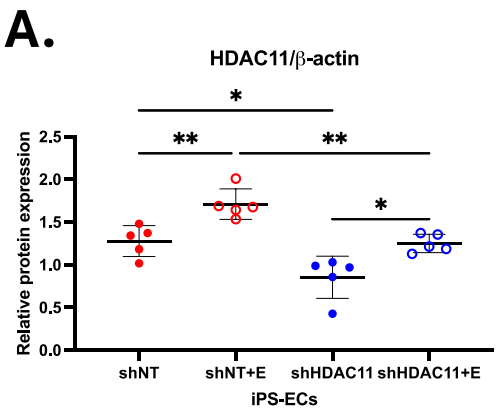

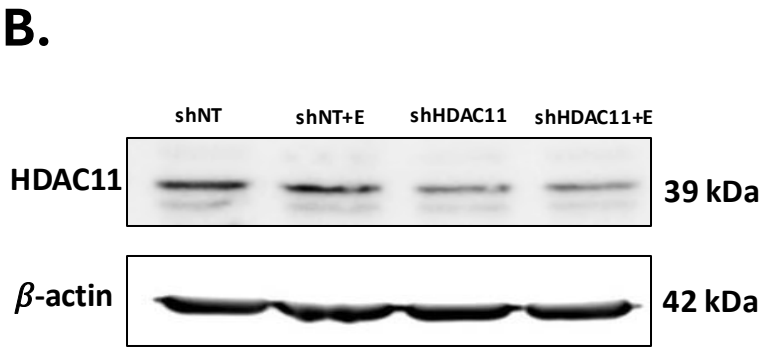

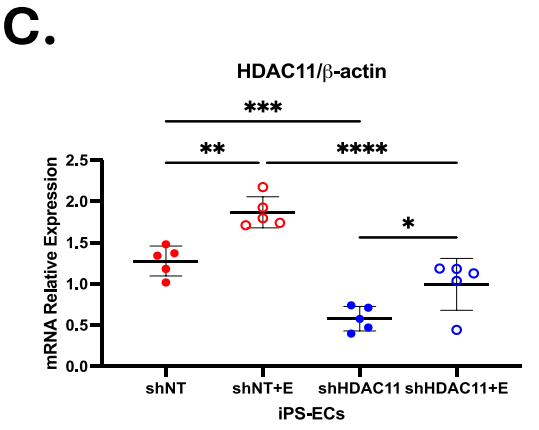

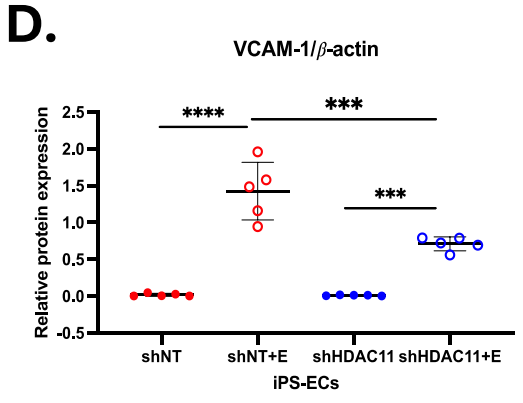

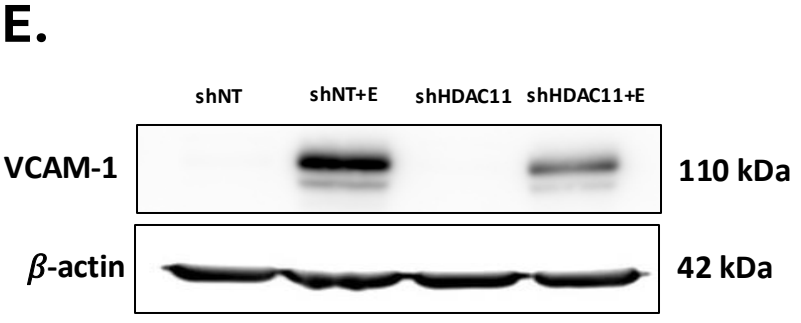

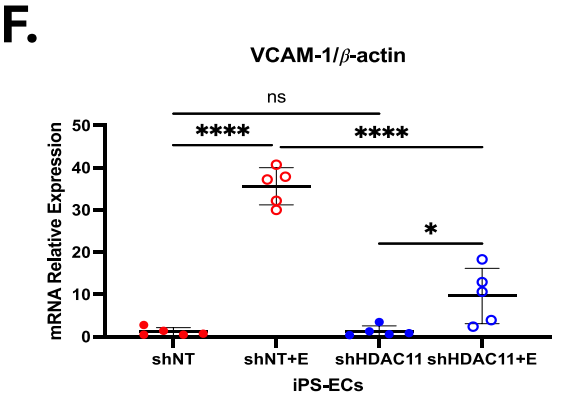

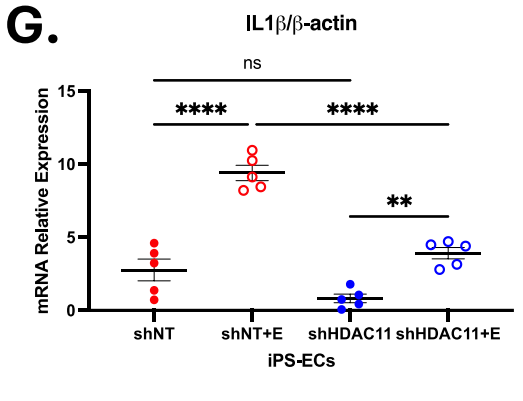

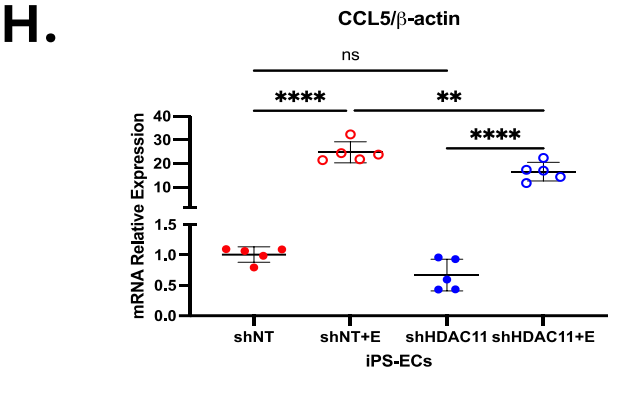

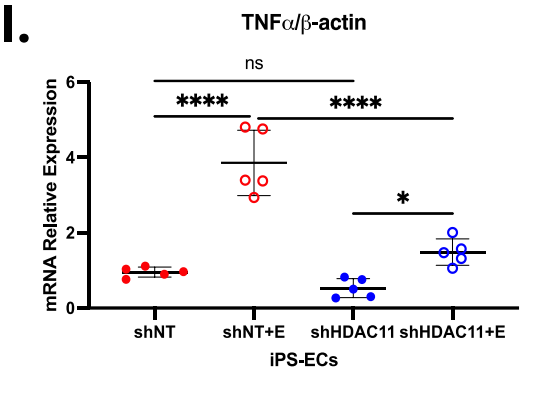

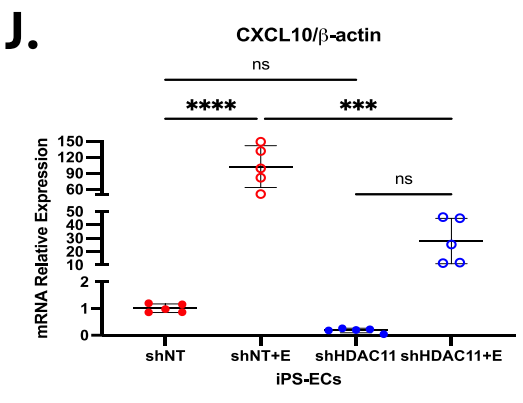

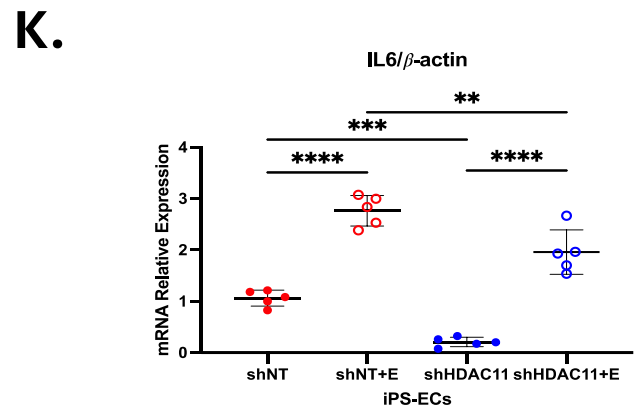

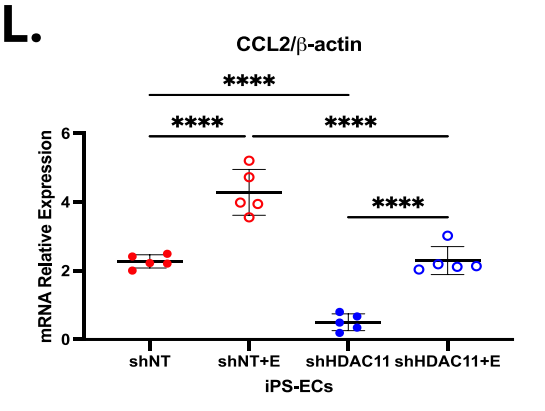

Supplementary figure 4. Knock down of HDAC11 using shRNA significantly reduces the production of the proinflammatory cytokines and chemokines. Knock down of HDAC11 significantly reduced the mRNA (A) and protein (B-C) expressions of HDAC11. E. coli infection enhanced the expression of HDAC11 however knock down of HDAC11 significantly reduced its expression. Moreover, the expression of VCAM-1 was not significantly affected by HDAC11 knockdown. However, following *E. coli* stimulation, the mRNA expression of VCAM-1 was lower in the shHDAC11 group compared to the shNT group **(D).** A representative image of VCAM-1 western blot **(E)**. **(F)** VCAM-1 protein expression was significantly reduced in the shHDAC11+E.coli compared to the shNT+E group. **(G-J)** The mRNA expression levels of IL1β, CCL5, TNFα, CXCL10, and CXCL6 remained constant upon HDAC11 knockdown. However, *E. coli* exposure increased mRNA expression of IL1β, CCL5, TNFα, CXCL10, IL6, and CCL2, knock down of HDAC11 reversed these expressions. **(K-L)** Additionally, IL6 and CCL2 expression decreased following HDAC11 knockdown. Upon *E. coli* exposure, the mRNA expression of IL6 and CCL2 significantly increased, while HDAC11 knockdown diminished this expression.

Statistical Significance: Statistical analysis was tested by Kruskall-Wallis or One-Way ANOVA, ✻ = $p < 0.05$ vs shNT; ✻✻ = $p < 0.01$ vs shNT; ✻✻✻ = $p < 0.001$ vs shNT; ✻✻✻✻ = $p < 0.0001$ vs shNT.

shNT = non-targeted shRNA, shNT+E = non-targeted shRNA+*E. coli* infection, shHDAC11 = HDAC11 knockdown, shHDAC11+E = HDAC11 knockdown+*E. coli* infection.

A.

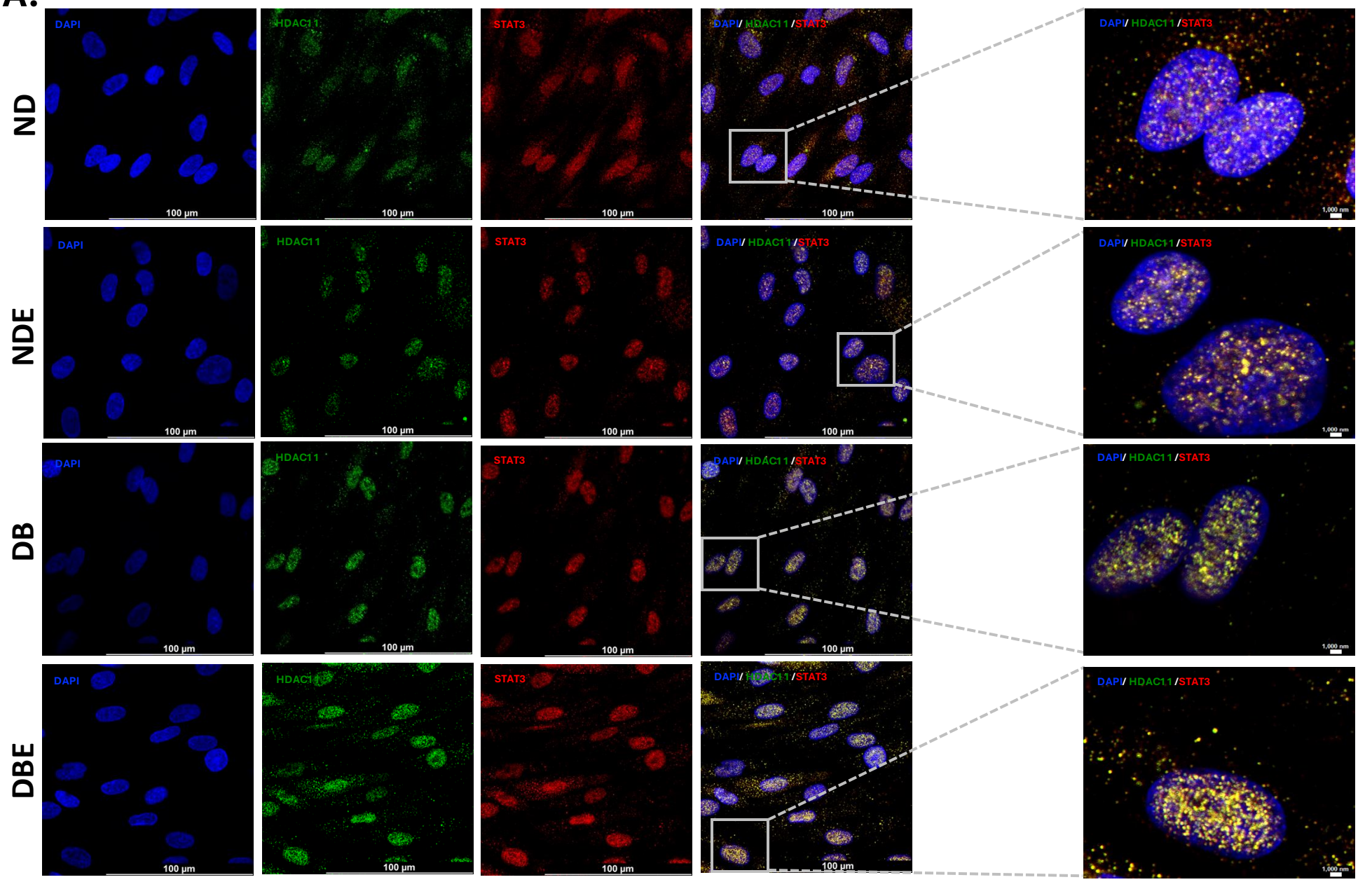

B.

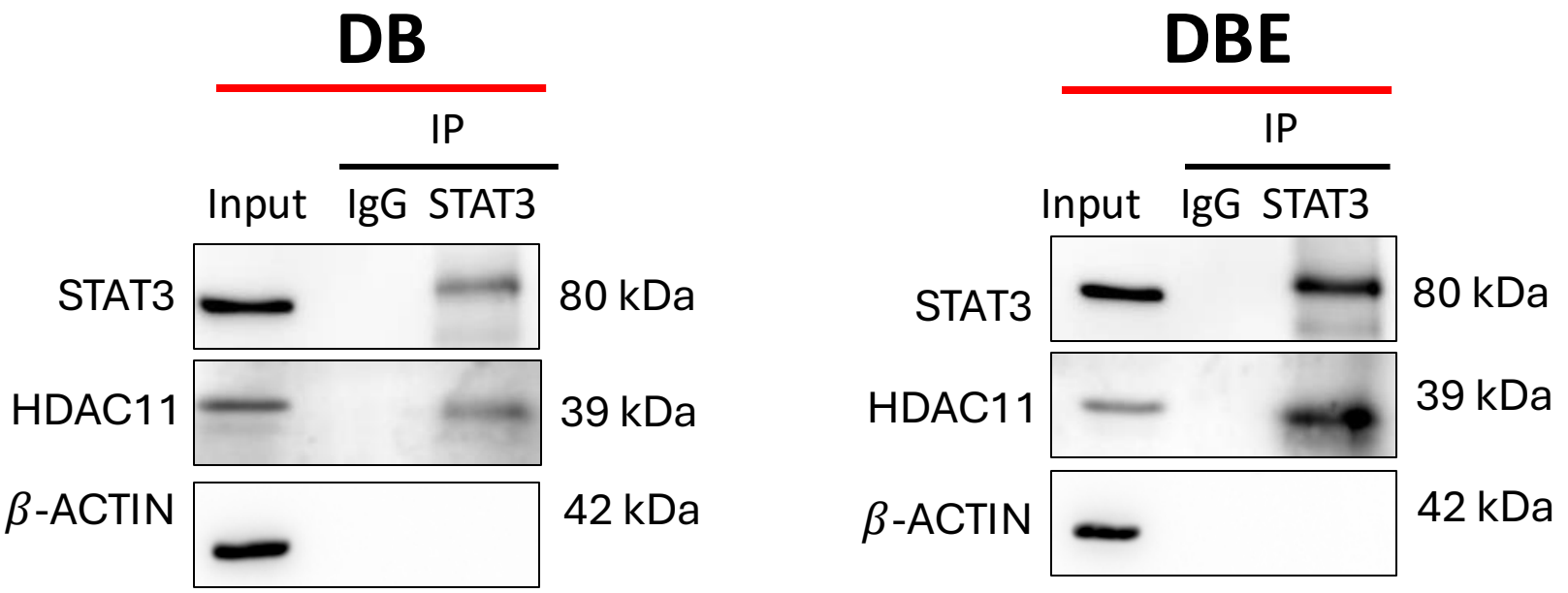

Supplementary figure 5. Upon *E. coli* infection, HDAC11 and STAT3 are expressed in the nucleus of the endothelial cells. (A) HDAC11 is predominantly expressed in the nucleus of the endothelial cells, although some fractions can be observed at the cytoplasm. Meanwhile. in the resting state, STAT3 was expressed at the nucleus and cytoplasm of the endothelial cells. However, in the presence of stimulation such as *E. coli*, STAT3 underwent translocation and predominantly expressed in the nucleus. **(B)** Interaction of HDAC11 in STAT3 in iPS-ECs derived from donors with diabetes. iPS-ECs were infected with *E. coli* for 2 hours and the cells were harvested at 48 hours post-infection. Immunoblot analysis of STAT3 immunoprecipitated (IP) with antibody to HDAC11. Mouse IgG was used as a negative control.
Imaging Details: Magnification: 63×; Scale bar: 100 µm.

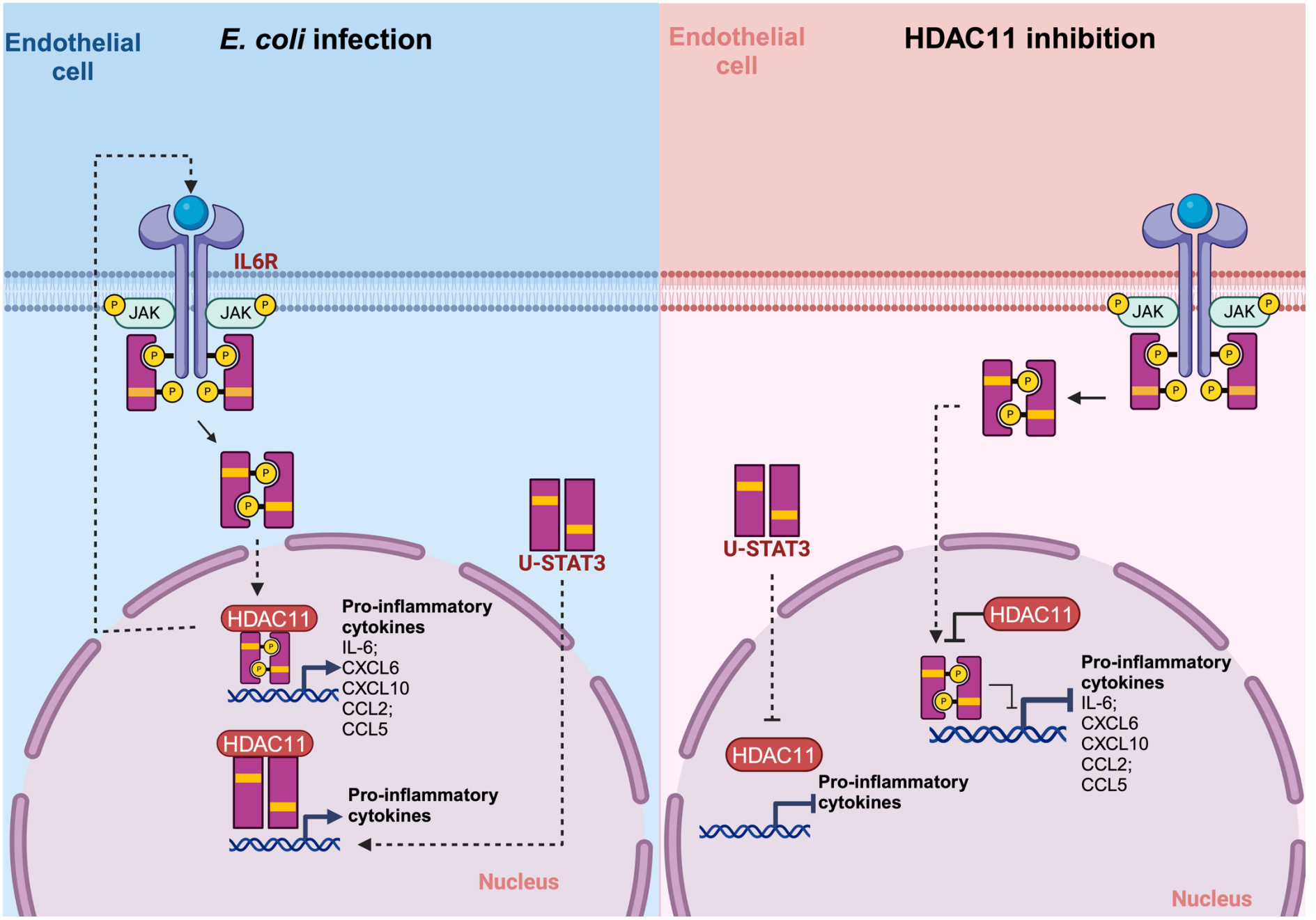

Supplementary figure 6. HDAC11 inhibition attenuates *E. coli*-induced inflammatory signalling in endothelial cells.
The left panel illustrates the IL6/JAK/STAT3 signalling cascade in endothelial cells upon *E. coli* infection, in which inducing the phosphorylation of STAT3 (pSTAT3) leading to translocation to the nucleus. In cooperation with HDAC11, this signalling enhances transcription of pro-inflammatory cytokines. Conversely, the right panel shows that inhibition of HDAC11 disrupts this signalling pathway by diminishing STAT3 nuclear translocation, thereby decreasing the transcription of pro-inflammatory cytokines. This mechanism highlights HDAC11 as a key regulator of EC inflammation in response to *E. coli* infection, particularly under comorbid conditions such as diabetes.